

# A Boost Test of Anomalous Diphoton Resonance at the LHC

Qing-Hong Cao,<sup>1,2,3,\*</sup> Yandong Liu,<sup>1,†</sup> Ke-Pan Xie,<sup>1,‡</sup> Bin Yan,<sup>1,§</sup> and Dong-Ming Zhang<sup>1,¶</sup>

<sup>1</sup>Department of Physics and State Key Laboratory of Nuclear Physics and Technology, Peking University, Beijing 100871, China

<sup>2</sup>Collaborative Innovation Center of Quantum Matter, Beijing 100871, China

<sup>3</sup>Center for High Energy Physics, Peking University, Beijing 100871, China

The recent observed diphoton resonance around 750 GeV at the LHC Run-2 could be interpreted as a weak singlet scalar. Adapting the approach of effective field theory we argue that the scalar might also decay into  $WW$  or  $ZZ$  pairs, which are highly boosted and appear as two fat vector-jets in the detector. We demonstrate that the signature of two vector-jets provides a powerful tool to crosscheck the diphoton anomaly and should be explored in the LHC Run-II experiment.

**Introduction:** Recently, an anomalous resonance around 750 GeV is observed in the diphoton channel at the level of  $3.9\sigma$  by the ATLAS collaboration and  $2.6\sigma$  by the CMS collaboration at the LHC Run-II [1, 2]. The observation stimulates great interests in the field [3–20]. It is attractive to interpret the diphoton resonance as a weak singlet scalar ( $S$ ) which democratically couples to gauge bosons in the Standard Model (SM) through a set of effective operators. There are only three such operators that couple the scalar  $S$  to pairs of vector bosons at the dimension five [21, 22]:

$$\begin{aligned} \mathcal{L}_{eff} = & \kappa_g \frac{S}{M_S} G_{\mu\nu}^a G^{a\mu\nu} + \kappa_W \frac{S}{M_S} W_{\mu\nu}^i W^{i\mu\nu} \\ & + \kappa_B \frac{S}{M_S} B_{\mu\nu} B^{\mu\nu}, \end{aligned} \quad (1)$$

where  $G_{\mu\nu}^a$ ,  $W_{\mu\nu}^i$  and  $B_{\mu\nu}$  denotes the field strength tensor of the  $SU(3)_C$ ,  $SU(2)_W$  and  $U(1)_Y$  gauge group, respectively. Note that the coefficients  $\kappa_{g,W,B}$  are expected to be around  $\mathcal{O}(M_S/\Lambda)$  with  $\Lambda$  being new physics scale beyond the capability of current LHC. Our study can be extended to the weak singlet pseudo-scalar whose couplings to gauge bosons arise from a Wess-Zumino-Witten anomaly term [23]. After symmetry breaking the SM gauge bosons are interwoven such that the  $S$  scalar will also decay into pairs of  $WW$ ,  $ZZ$ , and  $Z\gamma$ . Observing a resonance in the invariant mass spectrum of the  $WW$  ( $ZZ$ ) pair would consolidate the diphoton anomaly. The hadronic modes of the  $W$  and  $Z$  boson decay are preferred as they exhibit large branching ratios. On the other hand, the  $W$  or  $Z$  boson from the  $S$  decay is highly boosted such that the two partons from  $W$  and  $Z$  decays tend to be collimated and appear in the detector as one fat jet, named as a  $V$ -jet where  $V = W/Z$ . In this Letter we propose to utilize the so-called jet substructure method to probe the signature of boosted  $V$ -jets from the  $S$  decay in the process of  $pp \rightarrow S \rightarrow VV$  to crosscheck the diphoton excess.

**Scalar production and decay:** We adapt narrow width approximation (NWA) to parameterize the process of  $pp \rightarrow S \rightarrow XY$  as following

$$\sigma(pp \rightarrow S \rightarrow XY) = \sigma(pp \rightarrow S) \times \frac{\Gamma(S \rightarrow XY)}{\Gamma_S}, \quad (2)$$

where  $X$  and  $Y$  denote the SM gauge bosons while  $\Gamma_S$  the total width of the  $S$  scalar. The scalar can decay into five modes induced by the three effective operators. The partial widths of the  $S$  decay are listed as follows:

$$\begin{aligned} \Gamma(S \rightarrow gg) &= \frac{M_S}{\pi} 2\kappa_g^2, \\ \Gamma(S \rightarrow \gamma\gamma) &= \frac{M_S}{4\pi} (\kappa_W s_W^2 + \kappa_B c_W^2)^2, \\ \Gamma(S \rightarrow Z\gamma) &= \frac{M_S}{2\pi} (\kappa_W - \kappa_B)^2 (1 - r_Z)^3 c_W^2 s_W^2, \\ \Gamma(S \rightarrow WW) &\simeq \frac{M_S}{2\pi} (1 - 6r_W) \kappa_W^2, \\ \Gamma(S \rightarrow ZZ) &\simeq \frac{M_S}{4\pi} (\kappa_W c_W^2 + \kappa_B s_W^2)^2 (1 - 6r_Z), \end{aligned}$$

where  $r_V = m_V^2/M_S^2$ . For a 750 GeV scalar,  $r_V$  ( $\sim 0.01$ ) can be ignored in the above partial widths. We compare the branching ratio  $\Gamma(S \rightarrow XY)$  to  $\Gamma(S \rightarrow \gamma\gamma)$  in the following four special cases:

i)  $\kappa_B = 0$ ,

$$\begin{aligned} R_{WW} &\equiv \frac{\Gamma(S \rightarrow WW)}{\Gamma(S \rightarrow \gamma\gamma)} \sim 40, \\ R_{ZZ} &\equiv \frac{\Gamma(S \rightarrow ZZ)}{\Gamma(S \rightarrow \gamma\gamma)} \sim 12, \\ R_{Z\gamma} &\equiv \frac{\Gamma(S \rightarrow Z\gamma)}{\Gamma(S \rightarrow \gamma\gamma)} \sim 7; \end{aligned} \quad (3)$$

ii)  $\kappa_W = 0$ ,

$$R_{WW} = 0, \quad R_{ZZ} \sim 0.09, \quad R_{Z\gamma} \sim 0.6; \quad (4)$$

iii)  $\kappa_W = \kappa_B$ ,

$$R_{WW} = 2R_{ZZ} \sim 2, \quad R_{Z\gamma} = 0; \quad (5)$$

iv)  $\kappa_W = -\kappa_B$ ,

$$R_{WW} \sim 6.9, \quad R_{ZZ} \sim 1, \quad R_{Z\gamma} \sim 4.9. \quad (6)$$

Large  $R_{WW}$ ,  $R_{ZZ}$  and  $R_{Z\gamma}$  are needed to reach a good discovery in the processes of  $pp \rightarrow S \rightarrow WW/ZZ/Z\gamma$  at the LHC. We focus our attention on two cases of  $\kappa_B = 0$  and  $\kappa_W = -\kappa_B$  in this study and explore the  $V$ -jet

signature of the  $WW$  and  $ZZ$  modes. The study of  $Z\gamma$  mode will be presented elsewhere [24].

The process of interests to us is

$$pp \rightarrow S \rightarrow V(\rightarrow jj)V(\rightarrow jj). \quad (7)$$

For illustration we choose  $\kappa_g = \kappa_W = \kappa_B = 0.01$  as our benchmark parameters which yield the reference cross sections at the 14 TeV LHC and the scalar width as follows:

$$\begin{aligned} \sigma_0(WW) &= 57.91 \text{ fb}, & \sigma_0(ZZ) &= 28.37 \text{ fb}, \\ \sigma_0(\gamma\gamma) &= 31.05 \text{ fb}, & \Gamma_S^0 &= 0.07 \text{ GeV}. \end{aligned} \quad (8)$$

Taking advantage of the NWA, the cross section of  $pp \rightarrow S \rightarrow XX$  for other parameters can be obtained easily from the above benchmark cross sections from

$$\sigma(pp \rightarrow S \rightarrow XX) = \sigma_0(XX) \left(\frac{\kappa_g}{0.01}\right)^2 \left(\frac{g_{XX}}{0.01}\right)^2 \frac{\Gamma_S^0}{\Gamma_S}, \quad (9)$$

where

$$\begin{aligned} g_{WW} &= \kappa_W, \\ g_{ZZ} &= \kappa_W c_W^2 + \kappa_B s_W^2, \\ g_{\gamma\gamma} &= \kappa_W s_W^2 + \kappa_B c_W^2. \end{aligned} \quad (10)$$

Even though our study is based on the NWA, the results are valid for a large-width scalar, e.g.  $\Gamma_S = 0.06M_S \sim 45 \text{ GeV}$ .

**Collider simulation:** Now we turn to collider simulation. The  $W$  and  $Z$  bosons from the heavy scalar decay tend to be highly boosted. The distance of two partons from subsequent decay of  $W/Z$  can be estimated approximately as

$$\Delta R \sim 2M_V/p_T \sim 4M_V/M_S \sim 0.4 - 0.5, \quad (11)$$

where  $\Delta R_{ij} = \sqrt{(\eta_i - \eta_j)^2 + (\phi_i - \phi_j)^2}$  with  $\eta_i$  and  $\phi_i$  denoting the rapidity and azimuthal angle of parton  $i$ . Given such a smaller angular separation, the hadronic decay products from the  $V$ -boson would form a fat jet with a substructure in the detector. That yields a special collider signature of two fat  $V$ -jets. In order to mimic the signal events, the SM background should consist of  $W$  or  $Z$  bosons. We consider SM backgrounds as follows: i) the associated production of a  $W$  boson and multiple jets (denoted by  $W$ +jets); ii) the associated production of a  $Z$  boson and multiple jets ( $Z$ +jets); iii) the pair production of  $WW$ ,  $WZ$  and  $ZZ$  bosons; iv)  $t\bar{t}$  productions. The triple gauge boson productions are negligible after imposing all the cuts below.

We generate the signal process of  $pp \rightarrow S \rightarrow WW/ZZ$  and the background processes at the parton level using MadEvent [25] at the 14 TeV LHC and pass events to Pythia [26] for showering and hadronization. The

Delphes package [27] is used to simulate detector smearing effects in accord to a fairly standard Gaussian-type detector resolution given by  $\delta E/E = \mathcal{A}/\sqrt{E/\text{GeV}} \oplus \mathcal{B}$ , where  $\mathcal{A}$  is a sampling term and  $\mathcal{B}$  is a constant term. For leptons we take  $\mathcal{A} = 5\%$  and  $\mathcal{B} = 0.55\%$ , and for jets we take  $\mathcal{A} = 100\%$  and  $\mathcal{B} = 5\%$ . We also impose the lepton veto if the lepton has transverse momentum ( $p_T^\ell$ ) greater than 20 GeV, rapidity  $|\eta_\ell| \leq 2.5$  and its overlap with jets  $\Delta R_{j\ell} \geq 0.4$ . The missing transverse momentum ( $\cancel{E}_T$ ) is then defined to balance the total transverse momentum of visible objects. In our signal the missing transverse energy arises mainly from jet algorithm and energy resolution, therefore, those events containing missing energy more than 200 GeV are discarded.

A 2-pronged boosted  $V$ -jet is tagged using the so-called ‘‘mass-drop’’ technique with asymmetry cut introduced in Ref. [28]. The  $V$ -jet reconstruction is performed using Cambridge/Aachen algorithm with Fastjet [29]. The distance parameter of 1.2 is used to cluster a fat jet that is initiated by the boosted  $V$ -boson. We further require the invariant mass of the reconstructed  $V$ -jet ( $M_J$ ) within mass window [30]:

$$|M_J - M_V| \leq 13 \text{ GeV} \quad (12)$$

where  $m_W = 80.4 \text{ GeV}$  and  $m_Z = 91.2 \text{ GeV}$ . The  $V$ -jets in the signal events arise from the  $S$  scalar decay, therefore, they exhibit a  $p_T$  distribution peaking around  $M_S/2$  which is much harder than those  $V$ -jets from the SM backgrounds; see Figure 1(a) for the  $p_T$  spectrum of the reconstructed  $W$ -jet. We demand both the  $V$ -jets ( $J_{1,2}$ ) to satisfy

$$p_T(J_{1,2}) \geq 200 \text{ GeV}, \quad |\eta(J_{1,2})| \leq 3. \quad (13)$$

Furthermore, the two reconstructed  $V$ -jets are required to lie within the mass window

$$\Delta M_{JJ} \equiv |M_{J_1 J_2} - M_S| \leq 50 \text{ GeV}. \quad (14)$$

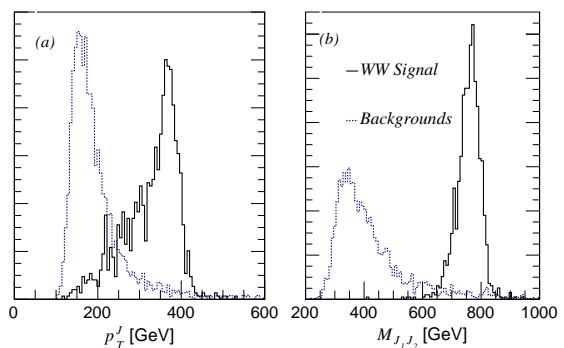


FIG. 1: The normalized distributions of the  $p_T$  of the reconstructed  $W$ -jet (a) and of the invariant mass of the two  $W$ -jets (b).

TABLE I: The numbers of the signal ( $\kappa_{g,W,B} = 0.01$ ) and background events after kinematic cuts at the 14 TeV LHC with an integrated luminosity of  $1 \text{ fb}^{-1}$ . The upper table is for the  $WW$  mode while the lower table for the  $ZZ$  mode.

	Signal	W+jets	Z+jets	$t\bar{t}$	WW	WZ	ZZ
No cut	57.91	1.7E8	4.98E7	5.5E5	9.54E4	4.36E4	1.25E4
W-jet	1.30	2158.96	630.30	67.22	64.87	23.45	8.98
$M_{JJ}$	1.03	185.21	45.02	8.25	8.51	3.29	1.09
	Signal	W+jets	Z+jets	$t\bar{t}$	WW	WZ	ZZ
No cut	28.37	1.7E8	4.98E7	5.5E5	9.54E4	4.36E4	1.25E4
Z-jet	0.60	1386.24	754.11	74.41	32.44	22.62	12.02
$M_{JJ}$	0.49	153.82	45.02	9.72	4.21	2.92	1.60

Figure 1(b) plots the invariant mass distribution of the two reconstructed  $W$ -jets in the  $WW$  channel. The numbers of the signal and the background events after all the above cuts are shown in the fourth and eighth rows of Table I with an integrated luminosity of  $1 \text{ fb}^{-1}$ . The signal event is calculated with our benchmark parameters,  $\kappa_{g,W,B} = 0.01$ , which serves merely for references. The cross section of other parameters can be derived easily from Eq. 9 and the numbers given in Table I. We emphasize that the cut efficiencies of the signal is not sensitive to the values of  $\kappa_{g,W,B}$  or the narrow width of the  $S$  scalar. After all the cuts the major background is from the productions of  $W$ +jets and  $Z$ +jets.

As the number of the signal and background events are large, we estimate the need cross section of the signal to claim a discovery from

$$\sigma_{\text{NV}} = \frac{5 \times \sqrt{\sigma_B}}{\epsilon_{\text{cut}} \times \sqrt{\mathcal{L}}}. \quad (15)$$

where  $\epsilon_{\text{cut}}$  denotes the cut efficiency of the signal. Figure 2 displays the discovery potential of the 750 GeV  $S$  scalar in the process of  $pp \rightarrow S \rightarrow WW$  (a, c) and  $pp \rightarrow S \rightarrow ZZ$  (b, d) at the 14 TeV LHC with an integrated luminosity of  $100 \text{ fb}^{-1}$  (dashed curve),  $300 \text{ fb}^{-1}$  (solid curve), and  $3000 \text{ fb}^{-1}$  (dot-dashed curve), respectively. The shaded green regions represent those parameter space consistent with the diphoton excess, which satisfy [1, 2]

$$\begin{aligned} \sigma_{\text{ATLAS}}(pp \rightarrow S \rightarrow \gamma\gamma) &\approx (10 \pm 3) \text{ fb}, \\ \sigma_{\text{CMS}}(pp \rightarrow S \rightarrow \gamma\gamma) &\approx (6 \pm 3) \text{ fb}. \end{aligned}$$

**Discussion:** First, thanks to the large  $R_{WW} \sim 40$  in the case of  $\kappa_B = 0$ , a  $5\sigma$  discovery of the  $pp \rightarrow S \rightarrow WW$  channel could be reached in the bulk of parameter space explaining the diphoton resonance at the 14 TeV LHC with an integrated luminosity of  $300 \text{ fb}^{-1}$ . If no excesses were observed, then the entire parameter space of diphoton anomaly would be excluded at the level of  $2\sigma$  with an integrated luminosity of  $100 \text{ fb}^{-1}$ ; see the red dashed curve in Fig. 2(a). On the other hand, the

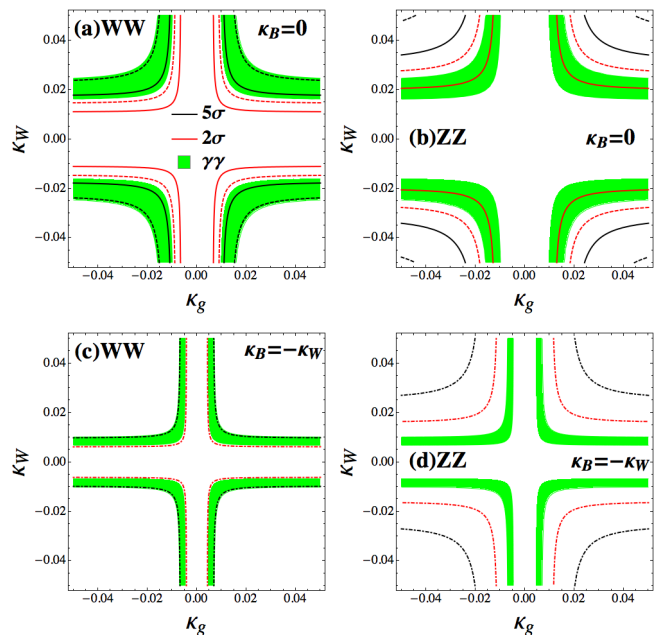


FIG. 2: The discovery potential of the process of  $pp \rightarrow S \rightarrow WW$  (a, c) and  $pp \rightarrow S \rightarrow ZZ$  (b, d) at the 14 TeV LHC with the integrated luminosity of  $100 \text{ fb}^{-1}$  (dashed curve),  $300 \text{ fb}^{-1}$  (solid curve), and  $3000 \text{ fb}^{-1}$  (dot-dashed curve). The shaded green region denotes the parameter space to explain the diphoton resonance. The black curves label the  $5\sigma$  discovery potential while the red curves represent the  $2\sigma$  exclusion.

$ZZ$  mode is less promising as the  $WW$  mode. The branching ratio of the  $ZZ$  mode is less enhanced as that of the  $WW$  mode such that only partial of the diphoton parameter space could be excluded by the  $ZZ$  mode with the integrated luminosity of  $300 \text{ fb}^{-1}$ .

Second, in the case of  $\kappa_W = -\kappa_B$ ,  $R_{WW} \sim 6.9$ . A large luminosity of  $3000 \text{ fb}^{-1}$  is needed to exclude the whole parameter space of diphoton anomaly in the  $WW$  mode; see the red dot-dashed curve in Fig. 2(c). Again, owing to  $R_{ZZ} = 1$ , the  $ZZ$  mode is not as good as the  $WW$  mode.

**Acknowledgement:** The work is supported in part by the National Science Foundation of China under Grand No. 11275009.

\* Electronic address: qinghongcao@pku.edu.cn

† Electronic address: ydliu@pku.edu.cn

‡ Electronic address: kpxie@pku.edu.cn

§ Electronic address: binyan@pku.edu.cn

¶ Electronic address: zhangdongming@pku.edu.cn

[1] The ATLAS Collaboration (2015), ATLAS-CONF-2015-081.

[2] The CMS Collaboration (2015), CMS-PAS-EXO-15-004.

[3] K. Harigaya and Y. Nomura (2015), 1512.04850.

- [4] Y. Mambrini, G. Arcadi, and A. Djouadi (2015), 1512.04913.
- [5] M. Backovic, A. Mariotti, and D. Redigolo (2015), 1512.04917.
- [6] A. Angelescu, A. Djouadi, and G. Moreau (2015), 1512.04921.
- [7] Y. Nakai, R. Sato, and K. Tobioka (2015), 1512.04924.
- [8] S. Knapen, T. Melia, M. Papucci, and K. Zurek (2015), 1512.04928.
- [9] D. Buttazzo, A. Greljo, and D. Marzocca (2015), 1512.04929.
- [10] A. Pilaftsis (2015), 1512.04931.
- [11] R. Franceschini, G. F. Giudice, J. F. Kamenik, M. McCullough, A. Pomarol, R. Rattazzi, M. Redi, F. Riva, A. Strumia, and R. Torre (2015), 1512.04933.
- [12] S. Di Chiara, L. Marzola, and M. Raidal (2015), 1512.04939.
- [13] T. Higaki, K. S. Jeong, N. Kitajima, and F. Takahashi (2015), 1512.05295.
- [14] S. D. McDermott, P. Meade, and H. Ramani (2015), 1512.05326.
- [15] J. Ellis, S. A. R. Ellis, J. Quevillon, V. Sanz, and T. You (2015), 1512.05327.
- [16] M. Low, A. Tesi, and L.-T. Wang (2015), 1512.05328.
- [17] B. Bellazzini, R. Franceschini, F. Sala, and J. Serra (2015), 1512.05330.
- [18] R. S. Gupta, S. Jger, Y. Kats, G. Perez, and E. Stamou (2015), 1512.05332.
- [19] C. Petersson and R. Torre (2015), 1512.05333.
- [20] E. Molinaro, F. Sannino, and N. Vignaroli (2015), 1512.05334.
- [21] Q.-H. Cao, C. B. Jackson, W.-Y. Keung, I. Low, and J. Shu, Phys. Rev. **D81**, 015010 (2010), 0911.3398.
- [22] I. Low, J. Lykken, and G. Shaughnessy, Phys. Rev. **D86**, 093012 (2012), 1207.1093.
- [23] G. Cacciapaglia, A. Deandrea, and M. Hashimoto, Phys. Rev. Lett. **115**, 171802 (2015), 1507.03098.
- [24] Q.-H. Cao, Y. Liu, K.-P. Xie, B. Yan, and D.-M. Zhang (2015), in preparation.
- [25] J. Alwall, P. Demin, S. de Visscher, R. Frederix, M. Herquet, F. Maltoni, T. Plehn, D. L. Rainwater, and T. Stelzer, JHEP **09**, 028 (2007), 0706.2334.
- [26] T. Sjöstrand, S. Ask, J. R. Christiansen, R. Corke, N. Desai, P. Ilten, S. Mrenna, S. Prestel, C. O. Rasmussen, and P. Z. Skands, Comput. Phys. Commun. **191**, 159 (2015), 1410.3012.
- [27] J. de Favereau, C. Delaere, P. Demin, A. Giammanco, V. Lematre, A. Mertens, and M. Selvaggi (DELPHES 3), JHEP **02**, 057 (2014), 1307.6346.
- [28] J. M. Butterworth, A. R. Davison, M. Rubin, and G. P. Salam, Phys. Rev. Lett. **100**, 242001 (2008), 0802.2470.
- [29] M. Cacciari, G. P. Salam, and G. Soyez, Eur. Phys. J. **C72**, 1896 (2012), 1111.6097.
- [30] G. Aad et al. (ATLAS) (2015), 1506.00962.